

Ageing of laser sintered glass-filled Polyamide 12 (PA12) parts at elevated temperature and humidity

Polymers and Polymer Composites

1–11

© The Author(s) 2021



Article reuse guidelines:

sagepub.com/journals-permissions

DOI: 10.1177/0967391211027127

journals.sagepub.com/home/ppc

Thomas Doohar¹ , Edward Archer¹, Tom Walls²,
Alistair McIlhagger¹ and Dorian Dixon¹

Abstract

Additive manufacturing is traditionally used to manufacture either prototypes or very small-scale demonstrators. In recent years though, it is being increasingly used to make low volume parts for the aeronautical and defence industry. One concern with laser sintered parts is that their relatively porous nature, means that they may be more susceptible to ageing than injection moulded parts. Parts were aged for 6 months in at different temperatures (18°C, 40°C, 50°C, 60°C, 80°C and 100°C) and in a humidity chamber at 60°C and 80% relative humidity. Each month samples were removed for characterisation. The testing included tensile testing, differential scanning calorimetry (DSC), thermogravimetric analysis (TGA), Fourier transform infrared spectroscopy (FTIR), Scanning Electron Microscopy (SEM) and gas pycnometry. During ageing the samples displayed visible discolouration and embrittlement over the 6-month test period. This embrittlement was not observed in those samples aged at room temperature or an elevated humidity. The observed yellowing in the samples aged above ambient temperature is likely a result of the build-up unsaturated degradation products. No significant differences as a result of ageing were observed via DSC, TGA, SEM or gas pycnometry.

Keywords

Ageing, PA12, laser sintered, mechanical properties, SLS

Received 30 March 2020; accepted 20 May 2021

Introduction

Additive manufacturing requires no tooling, complex shapes can be easily produced and costing is straightforward, based on the material and time required. However, 3D printing is much slower than alternative thermoplastic processing techniques and as such is poorly suited to high volume production. Even laser sintering which enables several parts to be produced simultaneously is still orders of magnitude slower than injection moulding. However, the use of additive manufacture in commercial production has increased in recent years, outside of the historical use in prototyping. For example, in the defence and aerospace sectors, companies including Boeing are using additive manufacture to produce low volume parts for the F18 fighter jet and 787 aircraft.^{1,2}

Weak interlayer/interparticle bonding and porosity may limit the mechanical performance of parts produced by such techniques. In the case of laser sintered components, incomplete bonding between particles, together with the presence of air pockets may reduce the mechanical properties as compared to solid extruded or moulded parts. Void levels of 2–10% depending upon the material choice and laser power have been previously reported for laser sintered PA12.³ However, in a comparison of laser sintered and injection moulded PA12, Van Hooreweder et al. reported that the ultimate tensile strength and tensile modulus were broadly similar for both production methods.³ While the strength and stiffness were similar for the two production methods, laser sintered parts were much more brittle with a reported elongation at break of 4–7% compared to 97% for injection moulded parts.⁴ In a separate study, it was reported that laser sintered PA12 parts

¹ School of Engineering, Ulster University, Newtownabbey, UK

² Laser Prototypes Europe, Belfast, UK

Corresponding author:

Dorian Dixon, School of Engineering, Ulster University, Shore Road, Newtownabbey BT37 0QB, UK.

Email: d.dixon@ulster.ac.uk

displayed a 35% and 10% increase in modulus and strength respectively over equivalent injection moulded parts but a reduction in impact performance. It was also reported that laser sintered PA12/carbon black composites displayed poorer mechanical performance than an equivalent injection moulded part.⁵

Additive manufacturing processes are often used to produce prototypes and there is limited data on the long-term in-service performance of parts.⁴ This is a particular issue for laser sintered parts, since the reported porosity will allow air and moisture to penetrate into the component, potentially accelerating ageing and degradation. Polyamides are the mostly widely employed materials for laser sintering, and it is widely acknowledged that these materials undergo significant degradation during ageing due to chain scission effects.⁶ Most of the published work on the degradation of polyamides is focused on PA6 and PA6,6 rather than the higher polyamides such as PA12 which are typically used in laser sintering. While it is known that polyamide materials absorb water, PA12 is somewhat less susceptible than the lower polyamides, due to the length of the alkane segments in the polymer structure. In PA12, the increase in ductility and toughness resulting from water uptake may be advantageous and for this reason some parts are submerged in water to accelerate water saturation.⁷ In one of the few published studies on the long-term performance of laser sintered parts, Goodridge et al., stored laser sintered PA12 parts at 20°C for 52 weeks in dry conditions, at 50%RH and totally submerged in water. It was reported that while the injection moulded samples showed little change over time, the laser sintered parts displayed a slight increase in tensile strength and Young's modulus over weeks 1–4. The laser sintered polyamide material was not found to be any more susceptible to the effects of room temperature ageing or moisture uptake than injection moulded parts.⁸ Seltzer et al., submerged PA12 and PA12 parts loaded with glass beads or ceramic short fibres in water at 90°C for 80 days. A reduction in tensile strength, modulus and toughness was observed after wet ageing. It was also noted that laser sintered parts have much lower elongation at break compared to moulded samples.⁹

In addition to water uptake, it is also known that polyamide degrades via oxidation which relies on diffusion from the surface leading to greater degradation nearer the surface.¹⁰ The presence of porosity in laser sintered parts is likely to enhance oxygen diffusion and may lead to a higher rate of degradation versus solid injection moulded components.

The Arrhenius relationship states that the rate of a chemical reaction increases exponentially with temperature. Since real time ageing at room temperature is impractical due to the time required, the Arrhenius relationship is often used in accelerated ageing studies, in which samples are stored at elevated temperatures (typically 50–60°C) for periods of several months, in order to mimic the effects of ageing for several years at room temperature.¹¹ However, at elevated temperatures, different ageing mechanisms can dominate which effects the validity of the results. For example, polypropylene shows curvature in the Arrhenius plot at 80°C and Polyurethane at 60°C. ASTM F1980-99 on the accelerated ageing of medical packaging, notes that a maximum ageing temperature of 60°C should be used. The standard also includes the proviso that the ageing should occur at least 10°C below the T_g (assuming that the service temperature experienced by the part is <T_g). It is important that a polymer is not aged above the T_g if the material is below T_g at ambient or service temperature, as this raises the likelihood of significant deviation from Arrhenius behaviour. The Arrhenius equation contains two constants which vary depending upon the material and frequently the value of these is not known. Therefore, the 10°C rule is often used industrially as a simplified alternative. This simplification assumes particular values for the Arrhenius constants, and is based on the estimation that the ageing rate doubles for every 10°C above room temperature (e.g. 6 months at 30°C is equivalent to 1 year at 20°C).

In this paper, we aim to build upon the existing knowledge by investigating the ageing of glass bead loaded laser sintered PA12. Glass loaded PA12 is widely used in laser sintering due to its excellent stiffness and strength over extended periods at a range of temperatures. Understanding the degradation behaviour at elevated temperature is vital for applications such as engine bay components where polyamide parts are widely used, and in the design of accurate accelerated ageing protocols. Dogbone shaped tensile testing specimens produced from 60% glass bead loaded PA12 via laser sintering, were aged at 18°C, 40°C, 60°C, 80°C and 100°C under ambient humidity and at 60°C and 80%RH, for a period of 6 months. Samples were removed from the ageing chambers at monthly intervals for testing and were characterised via tensile testing, TGA, DSC, FTIR, SEM and gas pyrometry.

Methods and materials

Sintered parts were produced by Laser Prototypes Europe (LPE) Ltd. The test specimens were produced using a commercial EOS P390 SLS printer with a build volume of 340 × 340 × 360 mm using general purpose commercial EOS PA2200 PA12 powder, filled with glass beads (60 wt%). The parts were sintered at a laser energy of 40 W with a scan speed of 4000 mm/s and a beam size of 0.64 mm. The dogbone parts were made according to the dimensions described in ISO-527 Type 5A. These were made along with parts from customers and as such are representative of actual production parts. The parts were then placed in ovens set at 40°C, 50°C, 60°C, 80°C and 100°C. Another batch of samples was placed in a humidity chamber set at 60°C and 80% relative humidity. A third batch was aged at room temperature (they were placed in a server room which is temperature controlled at 18°C). The samples were aged for 6 months, with six samples being removed every month for testing. Samples were also tested prior to ageing.

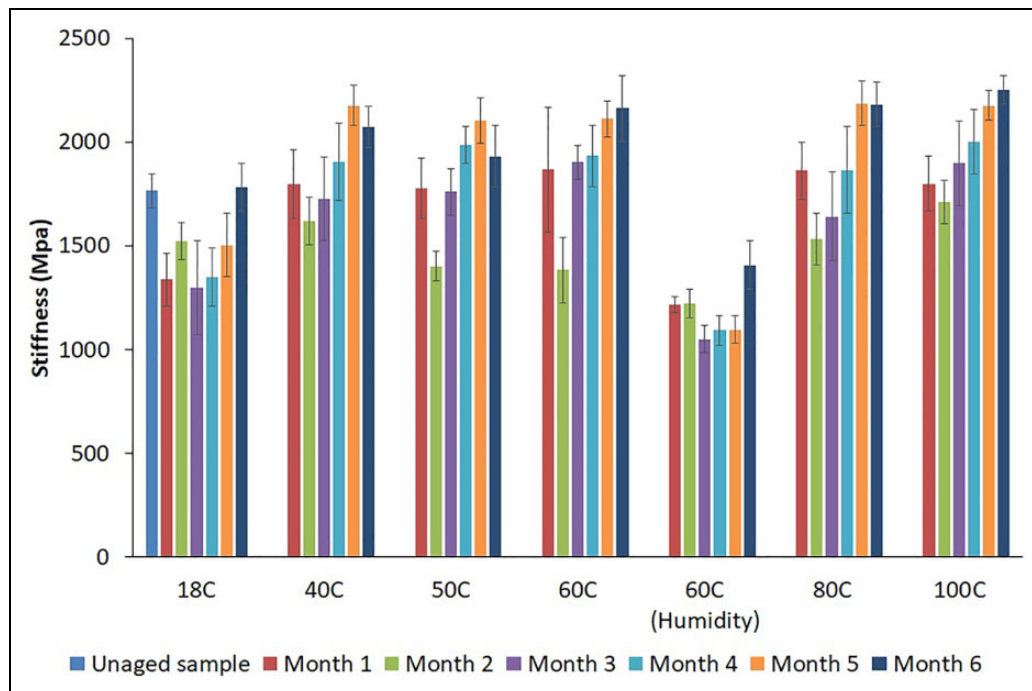


Figure 1. Effect of ageing on the stiffness.

Tensile testing was carried out using an Instron 3344 single column tensile tester at a crosshead speed of 5 mm/min. The load and displacement data were obtained from the tensile tester and analysed using Microsoft Excel. The Young's modulus, tensile strength, elongation at break and the energy at break were calculated.

Thermogravimetric analysis (TGA) was carried out using a TA instruments SDT Q600, under a nitrogen atmosphere (flow rate of 50 ml/min) at a heating rate of 10°C per minute from room temperature to 600°C. To measure the moisture content of the samples, the weight loss up to 150°C was used as some moisture may have penetrated deep into the material. The onset degradation temperature was calculated using TA instruments universal analysis software.

Differential scanning calorimetry was carried out using a TA instruments Q100 DSC. Tests were conducted from -90°C to 250°C at a heating rate of 10°C per minute, under a nitrogen atmosphere (flow rate of 50 ml/min). Analysis was conducted using TA instruments universal analysis software.

Fourier transform Infra-red (FTIR) spectroscopy was carried out using a Varian 610-IR FT-IR microscope using a Germanium crystal in ATR (Attenuated Total Reflectance) mode. Scans were run from 800 to 4000 cm^{-1} with a resolution of 4 cm^{-1} . The results were gathered using the integrated software (Agilent Resolutions Pro) and were converted and analysed using Microsoft Excel.

Gas pycnometry was carried using a Micromeritics AccuPyc II 1340 gas pycnometer with helium. This gave a measurement of the volume of the parts and was used to calculate the density. Approximately 1 cm^3 of material is required to achieve an accurate measurement. As a result, several of the fractured samples were used to obtain a measurement. This limited the number of available measurements to only one per batch. According to the manufacturer, the reproducibility is $\pm 0.02\%$ of the nominal full-scale volume.¹²

Scanning electron microscopy was carried out using a Joel JSM-6010 Plus/LV SEM at an acceleration voltage of 10 kV and the samples were gold sputter coated prior to analysis. The images were obtained in secondary electron mode, from the fractured surface of the samples after tensile testing.

Results and discussion

The Young's modulus, ultimate tensile strength and elongation at break results of the samples stored under the various conditions over a 6-month period are shown in Figures 1 to 3, respectively. The error bars in Figures 1 to 3 correspond to a 95% confidence interval ($\pm 1.96 \times$ standard error). The stiffness of the unaged sample at is 1.76 GPa is somewhat lower than the value of 2.43 GPa previously reported by Cano, for a laser sintered part made using PA12/40 wt% glass beads.¹³ This difference is likely to result from the use of different grades and production parameters. The tensile strength of the unaged sample is 27.8 MPa which is similar to the value of 29.3 MPa previously reported by Cano.¹³ While there is noticeable variation in the data, which may be due to the degree of variability inherent in laser sintered parts; the stiffness of the samples stored at evaluated temperature and ambient humidity tends to increase during ageing.

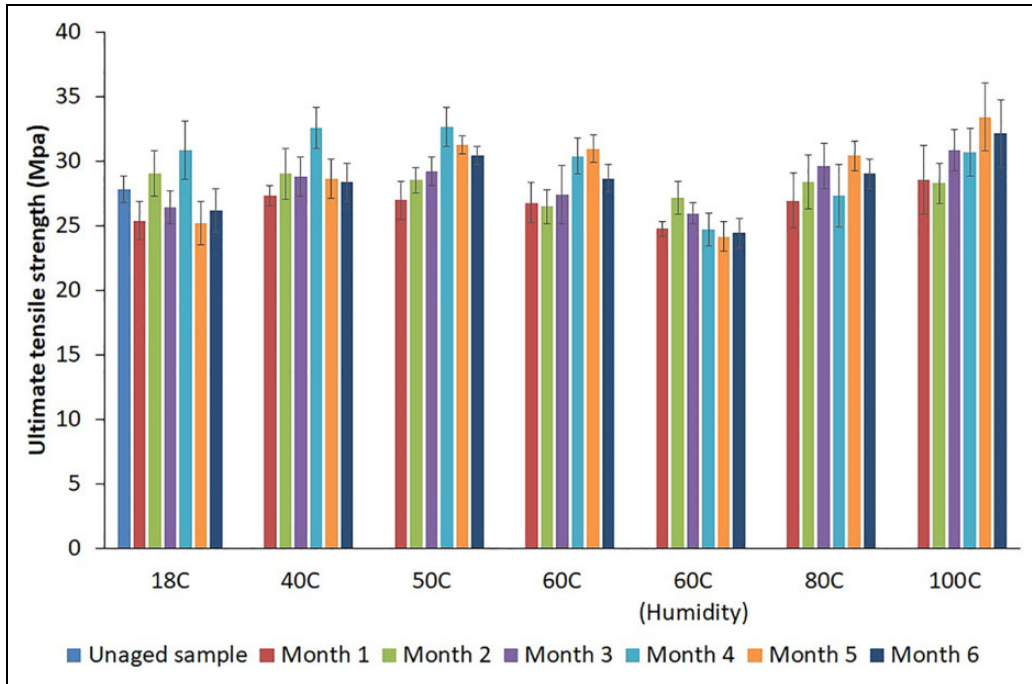


Figure 2. Effect of ageing on the ultimate tensile strength.

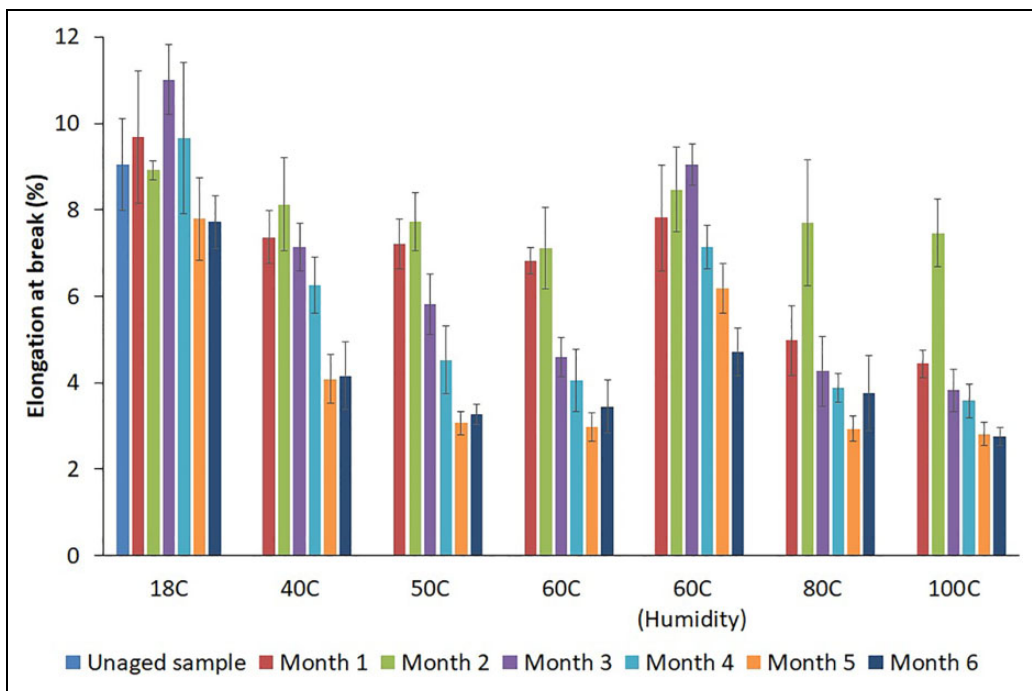


Figure 3. Effect of ageing on the elongation at break.

Referring to Figures 2 and 3, it is apparent that this increase in stiffness is accompanied by a corresponding reduction in elongation at break. The reduction in elongation at break is particularly notable, dropping from 9.0% for the unaged material to between 4.2% and 2.8% for those samples aged for 6 months between 40°C and 100°C. The fracture energy absorbed by the parts during the tensile tests (area under the stress/strain curves) was calculated as a measure of toughness. The energy absorbed during the failure of the unaged samples was 2.27 MJ/m³, which compares to 1.78, 1.01, 0.8, 0.8, 0.75 and 0.67 MJ/m³ for the samples aged at 18°C, 40°C, 50°C, 60°C, 80°C and 100°C, respectively. A corresponding value of 0.92 MJ/m³ was recorded for the samples aged at 60C and elevated humidity. It is known that water acts as a plasticiser in polyamides and increases toughness. The toughness of the samples are significantly lower

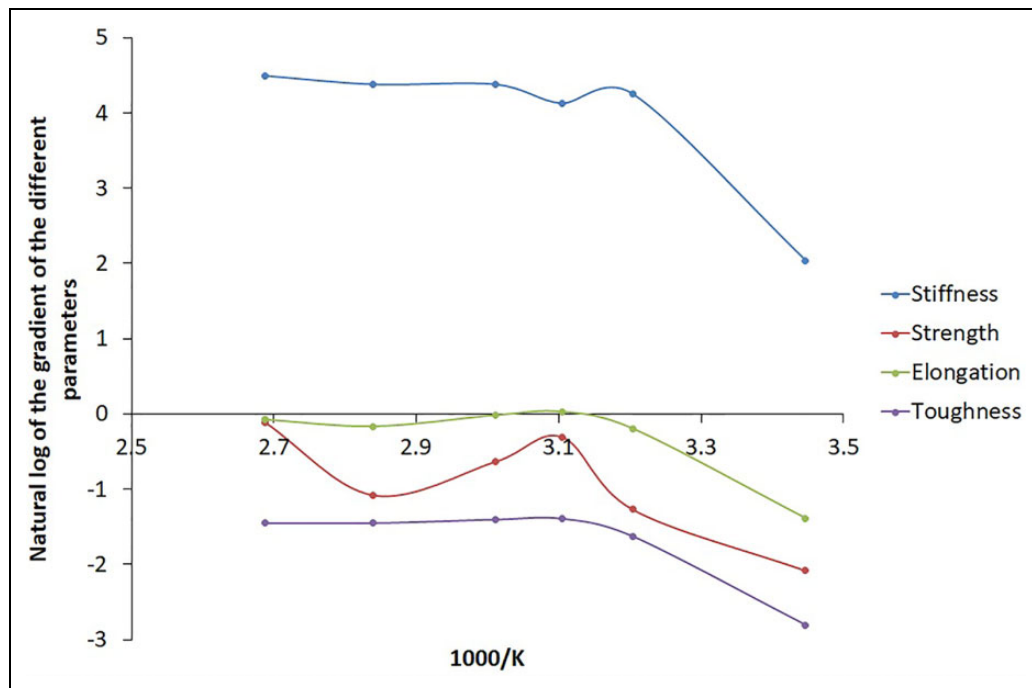


Figure 4. Arrhenius plot of the mechanical results.

than reported values for moulded pure PA12 (13 MJ/m³) which is likely due to the influence of laser sintering and the presence of the glass beads.¹⁴

These changes in the mechanical performance show that embrittlement is occurring during ageing. Such embrittlement after ageing, has previously been reported in various polyamides including PA6 and in polyamide copolymers.^{10,11,15,16} The thermal degradation of polyamides is a complex process with some debate over the location of the oxidative chain scission. For example, Straus and Wall suggested that degradation begins with the scission of the peptide C(O)–NH bonds,¹⁷ whereas Kamerbeek et al. assumed initial homolytic scission of the alkyl-amide NH–CH₂ bond.¹⁸ This oxidative process produces various low molecular weight fragments including caprolactam and may also lead to a degree of crosslinking.¹⁸ It is also widely recognised that physical ageing occurs in polyamides and in conjunction with oxidative degradation leads to embrittlement. Physical ageing refers to long-term changes in the local packaging of the chains polymers chains in the amorphous regions of rapidly cooled samples.¹⁹ Over time the material shrinks as the polymer chains rearrange, and while the process is temperature dependant it continues slowly even at room temperature. The increase in stiffness and reduction in elongation observed in the samples stored at 40°C, 50°C, 60°C, 80°C and 100°C did not occur in the samples aged at room temperature, with no statistically significant changes being observed in the samples stored at room temperature over the 6-month study period. PA12 has a glass transition temperature of ~36–43°C and in an ASTM standard (ASTM F1980-99) on the accelerated ageing of polymeric packaging, it was noted that if the polymer is below the glass transition temperature under service/ambient conditions, then one should conduct accelerated ageing at least 10°C below the T_g. This is due to the increased risk of deviation from Arrhenius behaviour if accelerated ageing is conducted above the T_g, if the part experiences temperatures below T_g in service. Some polymers such as PP and PE with a T_g below room temperature are both used and aged above their T_g. Depending upon the application, polymers such as PA12 may also subjected to a service temperature above the glass transition point. Using this ASTM guidance, the maximum recommended ageing temperature for PA12 is in the region of 26–33°C, for parts experiencing ambient service conditions. A material which displays Arrhenius ageing behaviour will show a linear relationship between the log of the variable being studied (i.e. stiffness) and the reciprocal of the temperature in Kelvin. It can be seen from the Arrhenius plot shown in Figure 4 that while the material generally displays Arrhenius behaviour between 40°C and 100°C, the materials aged at 18°C deviate from this. As previously discussed, this difference in the ageing behaviour at 18°C compared to the results obtained when ageing above 40°C is likely to result from the fact that the material is below the T_g at room temperature but is being ageing at or above the glass transition point. It is known that properties such viscosity and diffusion coefficient, change very significantly with temperature in the vicinity of the T_g.²⁰ These substantial changes can result in differing ageing mechanism dominating above and below the glass transition temperature, resulting in a discontinuity in the Arrhenius plot in the region of the T_g. For example, in a study of poly(vinyl acetate), Zhao and McKenna observed a discontinuity in the Arrhenius ageing behaviour above and below the T_g.²¹ Other researchers have reported the same behaviour.^{22–25} In a previous study we recommended a maximum ageing temperature for a PA12 based copolymer of ~45°C, since

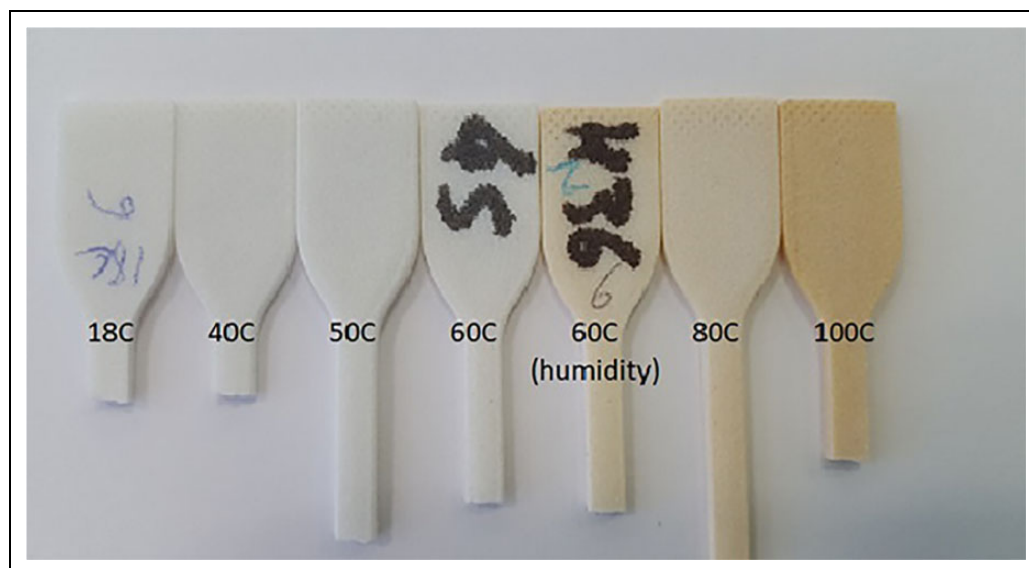


Figure 5. Discolouration of the samples after 6 months of ageing.

above this temperature the material displayed non-Arrhenius behaviour.¹¹ As previously noted, deviation from Arrhenius ageing has been reported at a range of temperatures for various polymers.⁶

Notable discolouration and yellowing was observed in the samples aged at higher temperature, as shown in Figure 5. This yellowing is commonly observed in the degradation of polyamides and has been previously attributed to the accumulation of unsaturated oligomer degradation products containing C=C bonds.²⁶ It is also seen that samples aged at 60°C at 80% RH display more yellowing than the samples aged at the same temperature under ambient humidity. It is widely understood that polyamides absorb water and due to that humidity influences the rate of polymer degradation. These interactions between water and polyamides are attributed to the presence of the amide group (-COHN), and it is known that these effects are less pronounced in higher polyamides than in PA6 or PA6,6 due to the lower amide group content. This has led to polyamides such as PA11 being used in water pipes.²⁶ Lower polyamides such as PA6 can absorb several weight percent of water which acts as a plasticiser lowering the Tg. For example, Khanna et al. reported a drop in the Tg of PA6 from 54°C at 0%RH to -28°C at 100%RH²⁷ while Jia et al. observed a reduction from 48°C at 0%RH to -19°C at 100%RH.²⁸ At higher temperatures it has been reported that elevated humidity increases the rate of degradation with Bernstein reporting that in the case of PA6,6 ageing, that thermooxidative degradation dominates below 50°C, while the effect of hydrolytic degradation is increasing important above this temperature.²⁹ An ageing study conducted in an oxygen free environment found that submerging PA11 samples in waters at temperatures of 110–140°C caused a significant loss in inherent viscosity due to chain scission and a resulting build-up in low molecular weight fragments.^{30–32}

The FTIR results are presented in Figure 6. All the main peaks associated with PA12 are apparent. The peak at 3300 cm^{-1} is attributed to the N–H stretch (belonging to hydrogen bonding).³¹ The peak at 3080 cm^{-1} is attributed to the N–H bond.³³ The peaks at 2920 is attributed to the CH₂ asymmetric stretching (reported at 2930 cm^{-1}) and 2848 cm^{-1} is attributed to the CH₂ symmetric stretching (reported at 2850 cm^{-1}).³⁴ The peaks between 2380 and 2310 cm^{-1} are attributed to the CO₂ bond between 2380 and 2320 cm^{-1} .^{30,33,35} The peak at 1640 cm^{-1} is attributed to the amide I band^{30–33,35} and the peak at 1550 cm^{-1} is attributed to the amide II band.^{30,31,36} The peak at 1460 cm^{-1} is attributed to CH₂ scissoring vibration³³ and the peak at 1365 cm^{-1} is attributed to CH bend, CH₂ twisting.⁶ Few significant differences are apparent in the spectra of the aged and unaged samples. However, there is evidence of the development of a more pronounced band at ~3090 cm^{-1} as a result of ageing. This band is attributed to C=C bonds, and the yellowing of Nylons has previously been attributed to the build-up of unsaturated degradation by-products such as cyclic or monomer oligomers.¹¹ The development of a similar C=C peak in this region was also observed in the high temperature ageing of a polyamide copolymer.⁹

Differential scanning calorimetry was carried out to see whether the ageing had any effect on either the glass transition temperature of the samples, or the crystallinity. The results can be seen in Figure 7 and Table 1. The weak feature at ~55°C in the unaged control sample is likely to correspond to the glass transition point but this is not visible in the aged samples. The presence of the glass beads will diminish the magnitude of the Tg signal. As shown in Table 1, there were no significant trends observed as a result of ageing in either the enthalpy of melt or the peak melting temperature. A reduction in the peak melt temperature would be expected if ageing produced in a large reduction in molecular weight as a result of chain scission.

Thermogravimetric analysis was used to see whether ageing caused any significant change in the degradation temperature of the polymer and whether there was any significant moisture absorption. The results can be seen in

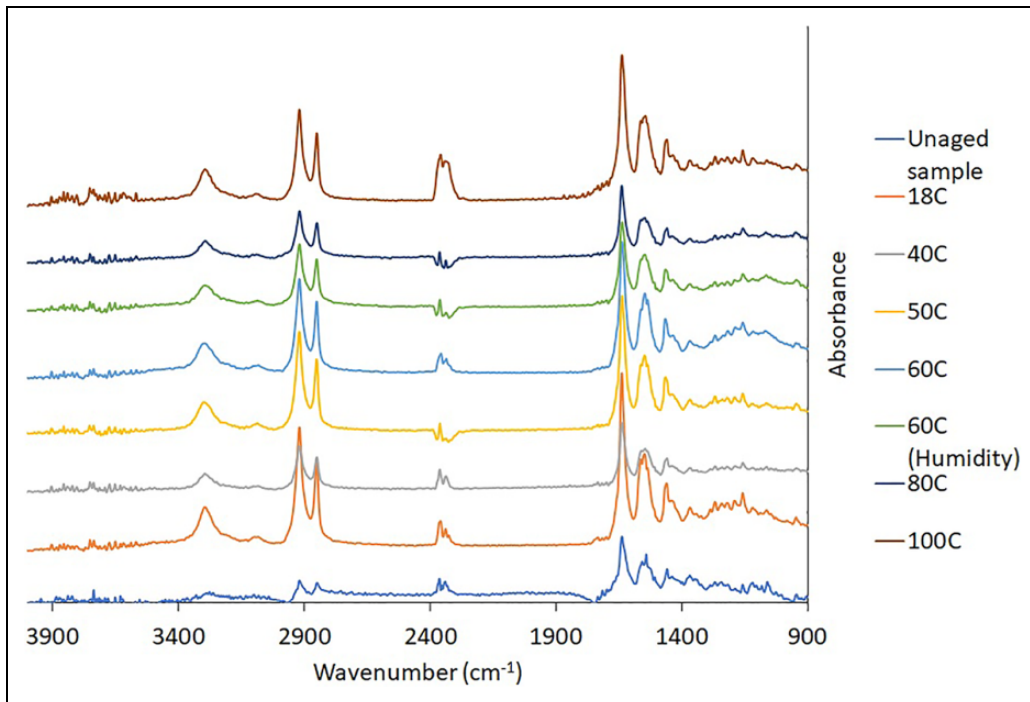


Figure 6. FTIR of the aged samples.

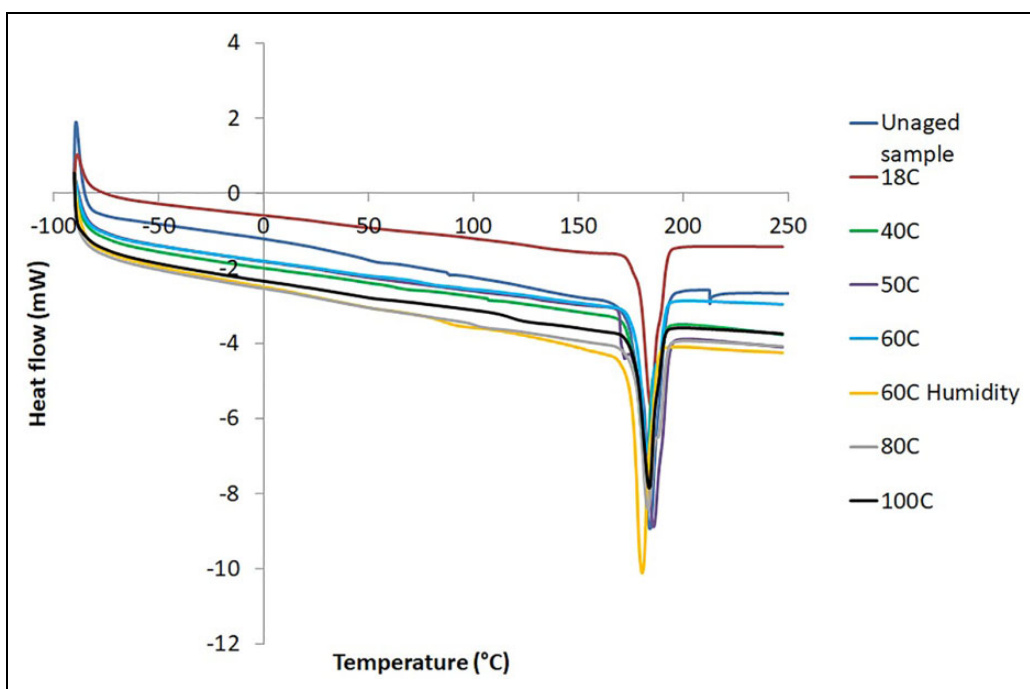
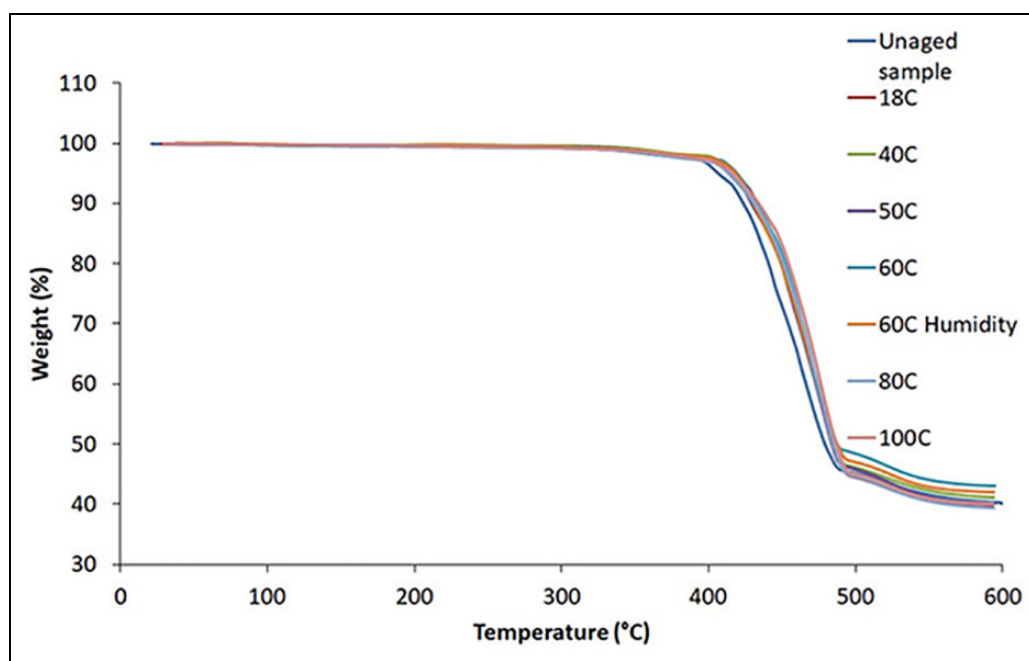


Figure 7. DSC of the aged samples.

Figure 8 and Table 2. The TGA curves match those in published work.³⁷ While there is some evidence of a degree of drying in the materials aged at elevated temperatures, only small variations were observed in moisture content between the samples stored at 18°C and those aged at elevated temperatures. The samples aged at 60°C and 80% RH generally show a slight increase in moisture content compared to those aged at 60°C and ambient humidity. Wingham et al. reported an initial water content of 0.14% for laser sintered PA12 parts which increased to 0.84% when the samples were subjected to steam autoclave conditions (steam at 121°C). One of the reasons why PA12 is used for laser sintering is due to its low moisture absorption compared to other polymers especially PA6.³⁸ While some variations in the onset degradation temperature were observed from sample to sample, no obvious changes were observed because of ageing.

Table 1. Enthalpy of melt and peak melting temperature of the aged materials.

Month	Enthalpy of melt (J/g)							Peak melting temperature (°C)						
	18°C	40°C	50°C	60°C	60°C (humid)	80°C	100°C	18°C	40°C	50°C	60°C	60°C (humid)	80°C	100°C
Unaged sample	44.16							184.1						
1	44.02	41.5	41.9	39.2	45.5	43.5	41.9	186.6	183.9	185.5	186.5	186.6	184.7	185.3
2	48.69	43.9	43.4	41.9	43.0	43.1	43.3	183.9	182.8	183.0	186.9	182.0	184.8	186.9
3	50.8	37.3	40.1	39.8	38.0	37.9	42.4	184.1	186.8	184.4	187.0	184.1	186.4	186.4
4	41.5	39.7	32.5	44.7	38.3	35.9	36.8	184.9	184.3	187.7	185.4	184.1	184.0	184.0
5	48.0	32.4	37.3	40.3	31.6	42.5	45.8	183.4	184.4	187.3	183.0	184.9	186.7	182.1
6	39.7	40.8	51.7	37.3	39.6	42.3	40.6	184.6	182.1	185.8	183.0	180.5	183.2	183.8

**Figure 8.** TGA of the aged samples.**Table 2.** Moisture content and onset degradation temperature of the aged materials.

Month	Moisture content (% of starting weight)							Onset degradation temperature (°C)						
	18°C	40°C	50°C	60°C	60°C (humid)	80°C	100°C	40°C	50°C	60°C	60°C (humid)	80°C	100°C	
Unaged sample	0.4							421.2						
1	0.1	0.3	0.3	0.1	0.2	0.1	0.1	420.9	427.2	424.4	426.7	421.1	428.5	428.9
2	0.2	0.2	0.2	0.3	0.3	0.2	0.2	432.8	430.4	431.8	424.8	428.2	422.7	428.0
3	0.3	0.2	0.2	0.3	0.5	0.2	0.2	434.6	433.3	435.7	434.8	435.9	437.4	439.1
4	0.3	0.2	0.2	0.3	0.4	0.2	0.4	427.1	425.4	427.9	428.7	432.1	434.4	436.5
5	0.3	0.1	0.1	0.1	0.4	0.2	0.1	426.4	421.6	423.5	420.8	424.1	422.2	417.3
6	0.3	0.2	0.3	0.3	0.4	0.2	0.2	428.4	428.9	431.6	436.4	427.0	435.4	438.5

The tensile fracture surface was studied using SEM and examples of typical micrographs of the samples aged for 6 months at 18°C and 100°C are shown in Figure 9. No obvious changes were observed in the SEM analysis of the samples aged at 40–100°C and at 60°C and elevated humidity compared to unaged material. The glass beads are clearly visible and are well distributed. It is also noted that no voids or porosity resulting from the SLS manufacturing process are visible.

The density of the parts after 6 months can be seen in Figure 10. There does appear to be some sample to sample variation in the density, and this variation of ~1% is likely due to natural variation in the parts. It is noted that ageing at elevated temperatures did not cause the particles to further consolidate within the parts.

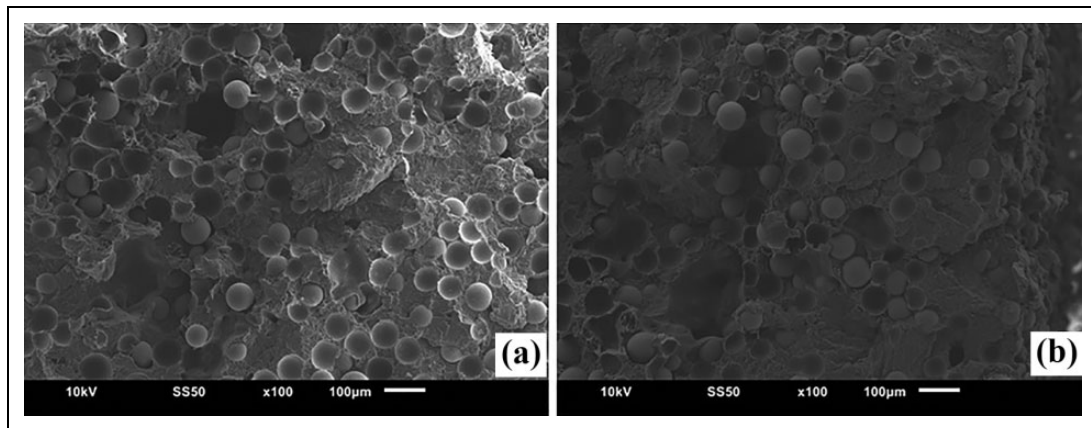


Figure 9. SEM of the aged samples after 6 months: (a) 18C and (b) 100C.

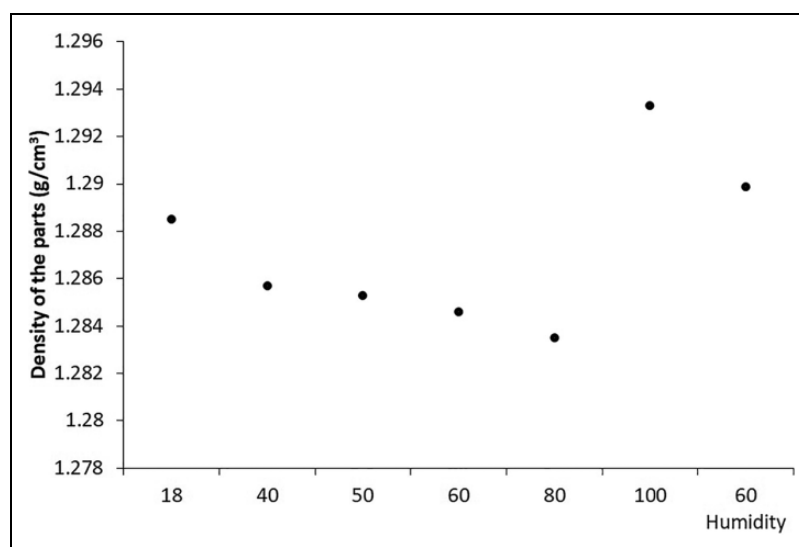


Figure 10. Density of the samples after 6 months.

Conclusions

Laser sintered glass-filled PA12 samples were supplied by Laser Prototypes Europe (LPE) and aged at 18°C, 40°C, 50°C, 60°C, 80°C and 100°C and in a humidity oven (60°C and at 80% RH) for 6 months. Samples were removed for testing each month. There was clear discolouration of the samples as a result of the ageing process which may be as a result of accumulated unsaturated degradation products.

Mechanical testing demonstrated that were becoming more brittle during ageing, as the elongation at break and toughness showed a decrease. Arrhenius plots showed that while there was a linear relationship between the samples aged at higher temperatures, the samples aged at 18°C did not share the same relationship. This was likely due to a shift in the ageing behaviour at glass transition temperature of PA12 which is between 36°C and 43°C. This limits the maximum temperature that can be reliably used during accelerated ageing studies.

Differential scanning calorimetry did not reveal any significant changes in the materials during the ageing process regardless of ageing time and temperature. The enthalpy of melt was measured for each sample tested to see whether there was a change which could point to a change in crystallinity, but no significant changes were observed. Neither was there a noticeable trend in the peak melting temperature.

Thermogravimetric Analysis (TGA) was also carried out to see whether there was evidence of moisture in the samples or whether there was a significant change in the chemical composition which would have changed the decomposition temperature of the samples. Only small differences in water content were observed between the samples stored under ambient conditions and those subjected to elevated temperature or humidity.

Scanning Electron Microscope (SEM) was carried out on the fractured surface of the samples aged after 6 months to see whether the ageing led to partial melting and an increase in the consolidation of the parts. There did not appear to be any significant differences observed between the samples, including those aged in the humidity chamber.

Finally, to see whether there was a change in the density of the samples, gas pycnometry was conducted after 6 months. It was found that there was no significant change in the density of the samples aged under different conditions.

Based on the information gathered it appears that laser sintered PA12 displays similar ageing characteristics to samples produced using other methods. The samples aged at elevated temperatures displayed an increase in embrittlement which was not seen in either room temperature aged samples. A distinct yellowing was also observed in the samples aged at higher temperatures.


Declaration of conflicting interests

The author(s) declared no potential conflicts of interest with respect to the research, authorship, and/or publication of this article.

Funding

The author(s) disclosed receipt of the following financial support for the research, authorship, and/or publication of this article: Funding for the project was provided by Invest NI through the Northern Ireland Advanced Engineering Competence Centre.

ORCID iD

Thomas Doher  <https://orcid.org/0000-0001-6866-3706>

References

1. Hartmann M. PA12—a new material for onshore, offshore and subsea applications | *15th Pipeline technology conference*. <https://www.pipeline-conference.com/abstracts/pa12-new-material-onshore-offshore-and-subsea-applications> (2015, accessed 22 May 2019).
2. Wudy K, Drummer D, Kühnlein F, et al. Influence of degradation behavior of polyamide 12 powders in laser sintering process on produced parts. In: *AIP conference proceedings*. American Institute of Physics, 2014, pp. 691–695.
3. van Hooreweder B, Moens D, Boonen R, et al. On the difference in material structure and fatigue properties of nylon specimens produced by injection molding and selective laser sintering. *Polym Test* 2013; 32: 972–981.
4. Dupin S, Lame O, Barrès C, et al. Microstructural origin of physical and mechanical properties of polyamide 12 processed by laser sintering. *Eur Polym J* 2012; 48: 1611–1621.
5. Athreya SR, Kalaitzidou K and Das S. Mechanical and microstructural properties of Nylon-12/carbon black composites: selective laser sintering versus melt compounding and injection molding. *Compos Sci Technol* 2011; 71: 506–510.
6. Levchik S V, Weil ED and Lewin M. Thermal decomposition of aliphatic nylons. *Polym Int* 1999; 48: 532–557.
7. Salmoria GV, Leite JL, Vieira LF, et al. Mechanical properties of PA6/PA12 blend specimens prepared by selective laser sintering. *Polym Test* 2012; 31: 411–416.
8. Goodridge RD, Hague RJM and Tuck CJ. Effect of long-term ageing on the tensile properties of a polyamide 12 laser sintering material. *Polym Test*. Epub ahead of print 2010. DOI: 10.1016/j.polymertesting.2010.02.009.
9. Seltzer R, de la Escalera FM and Segurado J. Effect of water conditioning on the fracture behavior of PA12 composites processed by selective laser sintering. *Mater Sci Eng A* 2011; 528: 6927–6933.
10. Gijsman P, Dong W, Quintana A, et al. Influence of temperature and stabilization on oxygen diffusion limited oxidation profiles of polyamide 6. *Polym Degrad Stab* 2016; 130: 83–96.
11. Dixon D and Boyd A. Degradation and accelerated ageing of poly(ether block amide) thermoplastic elastomers. *Polym Eng Sci* 2011; 51: 2203–2209.
12. AccuPyc II 1340 Specifications | Micromeritics. <https://www.micromeritics.com/CmsPage.aspx?contentpageid=5488&print=1> (accessed February 26, 2021).
13. Cano AJ, Salazar A and Rodríguez J. Effect of temperature on the fracture behavior of polyamide 12 and glass-filled polyamide 12 processed by selective laser sintering. *Eng Fract Mech* 2018; 203: 66–80.
14. Xu F, Yan C, Shyng YT, et al. Ultra-toughened nylon 12 nanocomposites reinforced with IF-WS2. *Nanotechnology* 2014; 25: 325701.
15. Shu Y, Ye L and Yang T. Study on the long-term thermal-oxidative aging behavior of polyamide 6. *J Appl Polym Sci* 2008; 110: 945–957.
16. El-Mazry C, Correc O and Colin X. A new kinetic model for predicting polyamide 6-6 hydrolysis and its mechanical embrittlement. *Polym Degrad Stab* 2012; 97: 1049–1059.
17. Straus S and Wall LA. Influence of impurities on the pyrolysis of polyamides. *J Res Nat Bureau Stand Sec A* 1959; 63A: 269.
18. Kamerbeek G, Kroes H and Grolle W. Thermal degradation of some polyamides. In: MacMillan New York (Eds) *Society of chemical industry monographs*, Vol. 13, 1961, p. 357.
19. Cowie JMG and Arrighi V. Physical aging of polymer blends. In: Utacki LA and White CA (Eds) *Polymer blends handbook*. Dordrecht: Springer Netherlands, 2014, pp. 1357–1394.
20. O'connell PA and McKenna GB. Relaxation in glassforming liquids and amorphous solids. *Liquid J Chem Phys* 1999; 110: 3113.
21. Zhao J and McKenna GB. Temperature divergence of the dynamics of a poly(vinyl acetate) glass: Dielectric vs. mechanical behaviors. *J Chem Phys* 2012; 136: 154901.

22. Celina M, Gillen KT and Assink RA. Accelerated aging and lifetime prediction: review of non-Arrhenius behaviour due to two competing processes. *Polym Degrad Stab* 2005; 90: 395–404.
23. Gijsman P, Hennekens J and Vincent J. The influence of temperature and catalyst residues on the degradation of unstabilized polypropylene. *Polym Degrad Stab* 1993; 39: 271–277.
24. Rosík L, Kovářová J and Pospíšil J. Lifetime prediction of ABS polymers based on thermoanalytical data. *J Ther Anal* 1996; 46: 465–470.
25. Gugumus F. Effect of temperature on the lifetime of stabilized and unstabilized PP films. *Polym Degrad Stab* 1999; 63: 41–52.
26. Romão W, Castro EVR, Filho EAS, et al. Ageing of polyamide 11 used in the manufacture of flexible piping. *J Appl Polym Sci* 2009; 114: 1777–1783.
27. Khanna YP, Kuhn WP and Sichina WJ. Reliable measurements of the nylon 6 glass transition made possible by the new dynamic DSC. *Macromolecules* 1995; 28: 2644–2646.
28. Jia N, Fraenkel HA and Kagan VA. Effects of moisture conditioning methods on mechanical properties of injection molded nylon 6. *J Reinf Plast Compos* 2004; 23: 729–737.
29. Bernstein R and Gillen KT. Nylon 6.6 accelerating aging studies: II. Long-term thermal-oxidative and hydrolysis results. *Polym Degrad Stab* 2010; 95: 1471–1479.
30. Ghosh S, Khastgir D, Bhowmick AK, et al. Thermal degradation and ageing of segmented polyamides. *Polym Degrad Stab* 2000; 67: 427–436.
31. Hnilica J, Potočnáková L, Stupavská M, et al. Rapid surface treatment of polyamide 12 by microwave plasma jet. *Appl Surf Sci* 2014; 288: 251–257.
32. Wan C, Zhao F, Bao X, et al. Effect of POSS on crystalline transitions and physical properties of polyamide 12. *J Polym Sci B Polym Phys* 2009; 47: 121–129.
33. Rhee S and White JL. Crystal structure and morphology of biaxially oriented polyamide 12 films. *J Polym Sci B Polym Phys* 2002; 40: 1189–1200.
34. Moshkovich M, Cojocar M, Gottlieb HE, et al. The study of the anodic stability of alkyl carbonate solutions by in situ FTIR spectroscopy, EQCM, NMR and MS. *J Electr Chem* 2001; 497: 84–96.
35. Novák I, Števiar M and Chodák I. Surface energy and adhesive properties of polyamide 12 modified by barrier and radio-frequency discharge plasma. *Monatsh Chem* 2006; 137: 943–952.
36. Cui X and Yan D. Preparation, characterization and crystalline transitions of odd–even polyamides 11,12 and 11,10. *Eur Polym J* 2005; 41: 863–870.
37. Vasquez M, Haworth B and Hopkinson N. Methods for quantifying the stable sintering region in laser sintered polyamide-12. *Polym Eng Sci* 2013; 53: 1230–1240.
38. Wingham JR and Omran MS. Effect of steam autoclaving on laser sintered polyamide 12. *Rapid Prototyp J* 2020; 27. Epub ahead of print 2020. DOI: 10.1108/rpj-11-2019-0288.